Polymer 55 (2014) 1666–1673

Contents lists available at ScienceDirect

Polymer

journal homepage: www.elsevier.com/locate/polymer

Pyridinyl-containing benzoxazine: Unusual curing behaviors with epoxy resins

Ching Hsuan Lin [a,*], Yu Sin Shih [a], Meng Wei Wang [a], Chun Yu Tseng [a], Tzu Chun Chen [a], Hou Chien Chang [a,*], Tzong Yuan Juang [b]

[a] Department of Chemical Engineering, National Chung Hsing University, Taichung 402, Taiwan
[b] Department of Applied Chemistry, National Chiayi University, Chiayi, Taiwan

ARTICLE INFO

Article history:
Received 1 December 2013
Received in revised form
5 February 2014
Accepted 9 February 2014
Available online 21 February 2014

Keywords:
Pyridinyl
Benzoxazine
Curing behaviors

ABSTRACT

A pyridinyl-containing benzoxazine (**6**) was synthesized from the Mannich condensation of 4-phenyl-2,6-bis(4-aminophenyl) pyridine (**2**), phenol, and paraformaldehyde. For the purpose of properties comparison, a benzoxazine (**7**), which is structurally similar to (**6**) except for the pyridinyl group, was prepared. The solvent effect on the synthesis of (**6**) was discussed, and toluene/ethanol was found to provide (**6**) with the best purity and yield. The pyridinyl group provides solubility and acts as a catalyst for the ring opening of benzoxazine, as supported by the forward curing in the DSC thermograms. When curing with epoxy resins, a carbonyl absorption at 1670 cm^{-1} and 192 ppm was observed in the IR and ^{13}C NMR spectra. It is proposed that the formation a cyclic amide structure is responsible for the absorption. A reaction mechanism including nucleophilic addition, Diels–Alder reaction, and rearrangement was proposed. The pyridinyl group acts as a crosslinking site, and results in thermosets with good thermal properties.

1. Introduction

Benzoxazines are resins that can be polymerized to thermosets by means of thermally activated ring-opening reactions, and have been reviewed by many authors [1–5]. Thermosets with low water absorption, superior electrical properties [6] and low surface energy [7] can be obtained after curing. There are two types of difunctional benzoxazines, including bisphenol-based benzoxazines, and diamine-based benzoxazines. Bisphenol-based benzoxazines are prepared by the condensation of bisphenol, primary monoamine, and formaldehyde. Diamine-based benzoxazines are prepared by the condensation of diamine, formaldehyde, and monophenol. It has been reported that incorporating pyridinyl groups into polymers can enhance solubility and thermal stability [8–13]. Therefore, we are interested in developing a pyridine-containing benzoxazine. Pyridinyl-containing amines are generally prepared by Chichibabin reaction [14–17] and modified Chichibabin reaction [18]. The diamines, 4-aryl-2,6-bis(4-aminophenyl) pyridines, can be prepared by a modified Chichibabin reaction [8]. In this work, we report the synthesis of a pyridinyl-containing benzoxazine (**6**) from the Mannich condensation of 4-phenyl-2,6-bis(4-aminophenyl) pyridine (**2**), phenol, and paraformaldehyde. A benzoxazine (**7**), which is structurally similar to (**6**) except for the pyridinyl group, was prepared for properties comparison. When (**6**) acts as an epoxy curing agent, unusual curing behaviors was found. Detailed synthesis of monomers, curing mechanism, and properties of the resulting thermosets are provided in this work.

2. Experimental part

2.1. Materials

Benzaldehyde, and paraformaldehyde were purchased from TCI. Phenol, ammonium acetate, and hydrazine hydrate 80%were purchased from Showa. Palladium on carbon 10%, p-nitroacetophenone were purchased from Acros. Glacial acetic acid and acetic anhydride were purchased from Scharlau. Boron trifluoride diethyl etherate was purchased from ALFA. Diglycidyl ether of bisphenol A (DGEBA) with an epoxy equivalent weight (EEW) of 187 g/eq and dicyclopentadiene epoxy (DCPDE, commercial name HP-7200) with EEW 269 g/eq were kindly supplied by Chang Chun Plastics, and Dainippon Ink and Chemicals Corporation, respectively. All solvents were HPLC grade and were purchased from Tedia.

* Corresponding authors.
E-mail address: linch@nchu.edu.tw (C.H. Lin).

http://dx.doi.org/10.1016/j.polymer.2014.02.039
0032-3861/

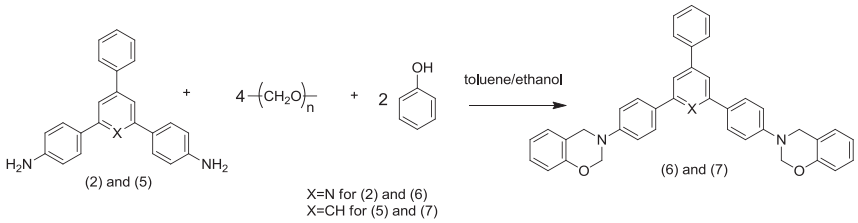

Scheme 1. Synthesis of benzoxazines (**6**–**7**).

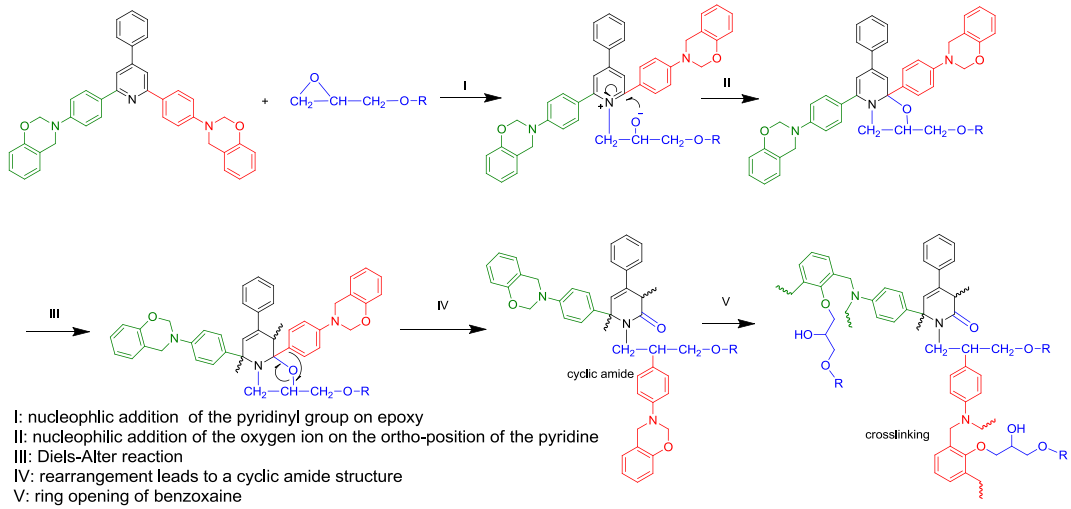

Scheme 2. The proposed reaction mechanism between (**6**) and epoxy.

2.2. Preparation of diamine (**2**)

Diamine (**2**) was prepared by a modified Chichibabin reaction, followed by reduction (Scheme S1, Supporting Information) [8]. ^{1}H NMR (ppm, DMSO-d_6), δ = 5.42 (4H, NH_2), 6.72 (4H, H^2), 7.48 (1H, H^{11}), 7.54 (2H, H^{10}), 7.81 (2H, H^6), 7.94 (2H, H^9), 8.04 (4H, H^3). ^{13}C NMR (ppm, DMSO-d_6), δ = 112.71(C^6), 113.66 (C^2), 126.57 (C^4), 127.04 (C^9), 127.75 (C^3), 128.82 (C^{11}), 128.97 (C^{10}), 138.56 (C^7), 148.62 (C^8), 149.85 (C^1), 156.60 (C^5). Melting point from DSC thermogram: 200.8 °C. Melting enthalpy 88.6 J/g.

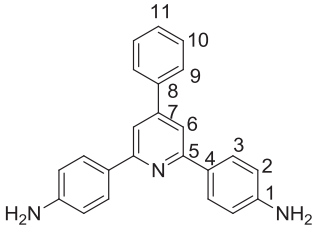

2.3. Preparation of diamine (**5**)

Diamine (**5**) was prepared by a three-step procedure according to the literature (Scheme S2, Supporting Information) [19]. ^{1}H NMR (ppm, DMSO-d_6) δ = 5.2 (4H, NH_2), 6.7 (4H, H^2), 7.4–7.5 (7H, $H^{3,10,11}$), 7.5–7.8 (5H, $H^{6,9,12}$). Melting point from DSC thermogram: 229.3 °C. Melting enthalpy 77.5 J/g.

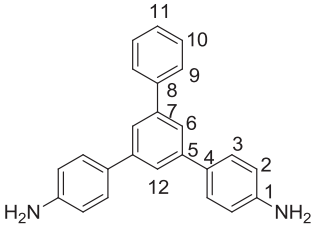

Table 1
Solvent effects on benzoxazine synthesis.

Run	Sample ID	Temp (°C)	Time (h)	Solvent	Reaction status
1	(**6**)	80	24	1,4-dioxane	A lot of gelation
2	(**6**)	80	24	xylene	A lot of gelation
3	(**6**)	80	24	toluene	A lot of gelation
4	(**6**)	60	24	chloroform	Homogeneous but low yield
5	(**6**)	80	24	1,4-dioxane/ ethanol (2:1)	Homogeneous but low yield
6	(**6**)	80	24	xylene/ ethanol (2:1)	Homogeneous but low yield
7	(**6**)	80	24	toluene/ ethanol (2:1)	Homogeneous with high yield
8	(**7**)	60	24	chloroform	Powder precipitation during polymerization
9	(**7**)	80	24	toluene/ ethanol (2:1)	Powder precipitation during polymerization
10	(**7**)	80	24	toluene/ ethanol (1:1)	Powder precipitation during polymerization

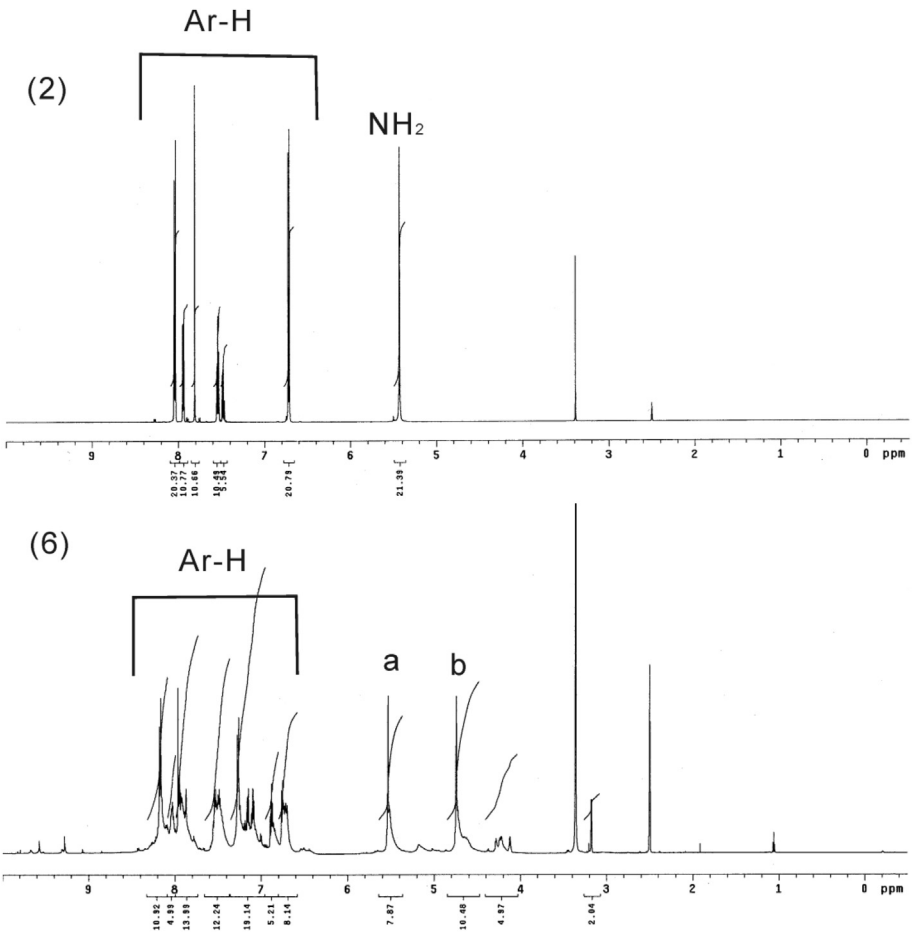

Fig. 1. ^{1}H NMR spectra of (**2**) and (**6**) in DMSO-d_6.

2.4. Synthesis of benzoxazines (**6**–**7**)

Benzoxazine (**6**) was prepared by a one-pot procedure (Scheme 1). (**2**) 3.00 g (9 mmol), phenol 1.6735 g (18 mmol), paraformaldehyde 1.068 g (36 mmol), and a mixed solvent of toluene/ethanol 30 mL (2/1, V/V) were introduced into a round-bottom 100 mL glass flask equipped with a nitrogen inlet, a condenser, and a magnetic stirrer. The reaction mixture was stirred at 80 °C for 24 h. After that, the solution was poured into methanol. The precipitate was filtered and dried in a vacuum oven. Yellow powder (80% yield) was obtained. Benzoxazine (**7**) was similarly prepared except the starting diamine is (**5**). Yellow powder (90% yield) was obtained.

2.5. Preparation of benzoxazine/epoxy thermosets

Since the pyridinyl group also reacted with epoxy resins (to be discussed in Scheme 2), the equivalent weight of benzoxazine (**6**) is one-third of its molecular weight. Benzoxazine/epoxy thermosets were prepared from an equivalent amount of (**6**) and epoxy resins (DGEBA and DCPDE). The mixture was stirred at 140 °C and transferred to an aluminum mold, and then cured at 160, 180, 200 and 220 °C for 2 h each in an air-circulating oven. Thereafter, samples were allowed to cool slowly to room temperature to prevent cracking. The sample ID is referred to as the (**6**)/DGEBA and (**6**)/DCPDE thermoset, respectively.

2.6. Characterization

Differential scanning calorimetry (DSC) was performed using a Perkin–Elmer DSC 7 in a nitrogen atmosphere at a heating rate of 10 °C/min. Thermal gravimetric analysis (TGA) was performed with a Perkin–Elmer Pyris1 at a heating rate of 20 °C/min in a nitrogen or air atmosphere. Dynamic mechanical analysis (DMA) was performed with a Perkin–Elmer Pyris Diamond DMA with a sample size of 2.0 × 1.0 × 0.2 cm. The storage modulus E′ and

Table 2
Solubility data of benzoxazines (**6**–**7**).[a]

Sample ID	Solvent									
	NMP	DMAc	DMF	DMSO	Dioxane	CH_2Cl_2	$CHCl_3$	THF	Toluene	Xylene
(**6**)	+	+	+	+	+	+	+	+	±	±
(**7**)	±	±	±	±	±	±	±	±	−	−

+, soluble; +h, soluble on heating; ±, partially soluble on heating; −, insoluble on heating.
[a] Solubility was tested with a 10 mg sample in 1 mL of solvent.

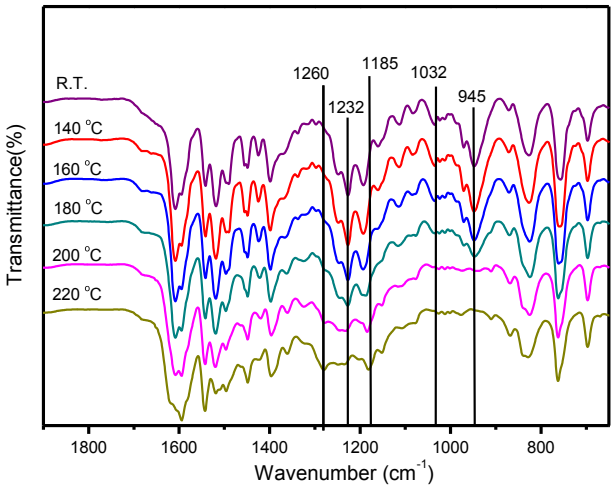

Fig. 2. IR spectra of (**6**) after accumulative curing at each temperature for 20 min.

tan δ were determined as the sample was subjected to the temperature scan mode at a programmed heating rate of 5 °C/min at a frequency of 1 Hz. The test was performed using a bending mode with an amplitude of 5 μm. Thermal mechanical analysis (TMA) was performed with a Perkin–Elmer Pyris Diamond TMA at a heating rate of 5 °C/min. NMR measurements were performed using a Varian Inova 600 NMR in DMSO-d_6, and the chemical shift was calibrated by setting the chemical shift of DMSO-d_6 as 2.49 ppm. The infrared spectra were recorded using a Nicolet Avatar 320 FTIR spectrophotometer. IR Spectra were obtained from at least 32 scans in the standard wavenumber range of 400–4000 cm^{-1} by a Perkin–Elmer RX1 infrared spectrophotometer.

3. Results and discussion

3.1. Synthesis of benzoxazine (6)

Benzoxazine (**6**) was prepared from the Mannich condensation of (**2**), paraformaldehyde, and phenol (Scheme 1).

Table 1 lists the solvent effect on the synthesis of (**6**). Using homo-solvents, such as 1,4-dioxane (Run 1), xylene (Run 2), and toluene (Run 3) led to insoluble gelation. Homogeneous solution can be achieved using chloroform (Run 4) and mixed solvents such as 1,4-dioxane/ethanol (Run 5), xylene/ethanol (Run 6), and Toluene/ethanol (Run 7). Among these solvents, toluene/ethanol

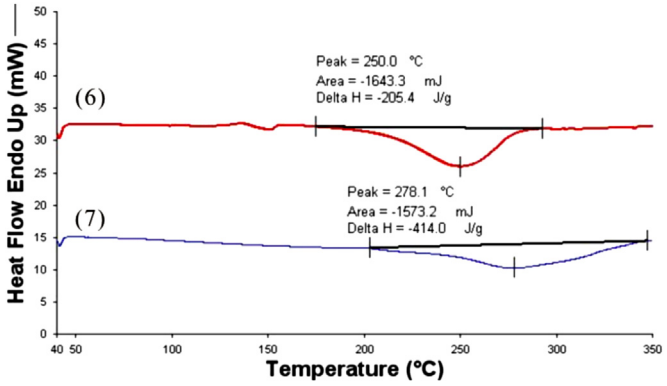

Fig. 3. DSC thermograms of benzoxazines (**6**) and (**7**).

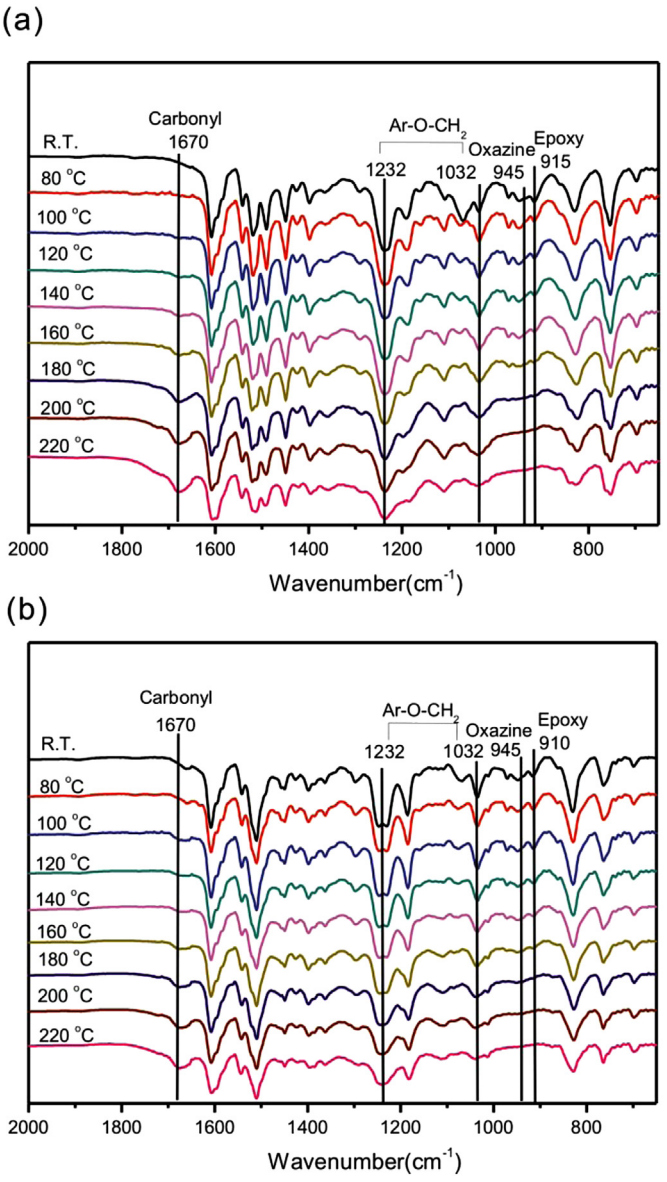

Fig. 4. IR spectra of (a) (**6**)/DGEBA and (b) (**6**)/DCPDE after accumulative curing at each temperature for 20 min.

(2/1, V/V) (Run 7) gave the best purity and yield. In our previous work [20], we proposed that the solvation effect of ethanol enhances the solubility of benzoxazine. This strategy also works effectively in this study. Fig. 1 shows the NMR spectra of (**2**) and (**6**) prepared by Run 7. The amino peaks of (**2**) disappeared completely, and new peaks a and b for oxazine were observed at 4.6 and 5.5 ppm. However, signals of impurity at 9.2–9.8 ppm and 4.0–4.5 were observed in (**6**), probably due to partially ring-opened structure of (**6**). Recently, Endo et al. reported the preparation of 1,3-benzoxazine bearing 4-pyridyl group, and found viscous substance. They speculated that the viscous product was a resole-type byproduct, of which formation was promoted by highly basic 4-aminopyridine [21]. Therefore, the impurity in Fig. 1 might also be related with the basicity of pyridinyl group. In the IR spectrum, absorptions at 945 cm^{-1} for oxazine, and absorptions at 1032 cm^{-1} (symmetric stretch) and 1232 cm^{-1} (asymmetric stretch) for Ar–O–C were observed, supporting the structure of (**6**).

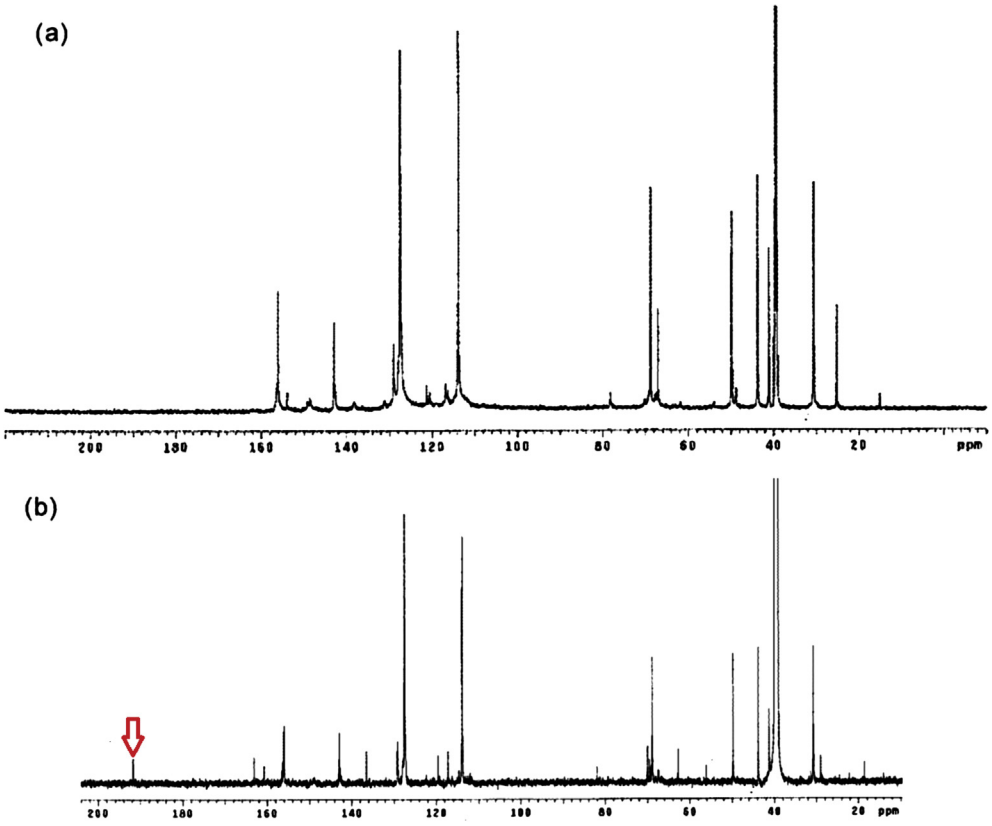

Fig. 5. ^{13}C NMR spectrum of (**6**)/DGEBA after curing at (a) 140 and (b)180 °C for 20 min.

3.2. Synthesis of benzoxazine (7)

Diamine (**5**), a precursor for benzoxazine (**7**) synthesis, was prepared by a three step procedure [19]. Benzoxazine (**7**) was prepared from the Mannich condensation of (**5**), paraformaldehyde, and bisphenol A (Scheme 1 and Table 1 Run 8–10). In contrast to the good solubility of (**6**), preparing benzoxazine (**7**) in chloroform (Run 8) and toluene/ethanol (Runs 9–10) results in powder precipitate (not gelation) after 1 h due to the poor solubility of (**7**), which limits the purity of (**7**). Fig. S1 shows the ^{1}H NMR spectra of (**5**) and (**7**). The amino peaks of (**5**) at 5.2 ppm disappeared completely, while new peaks a and b for oxazine were observed at 4.7 and 5.5 ppm. Table 2 lists the solubility of (**6**) and (**7**). While pyridinyl-containing (**6**) shows good solubility in several

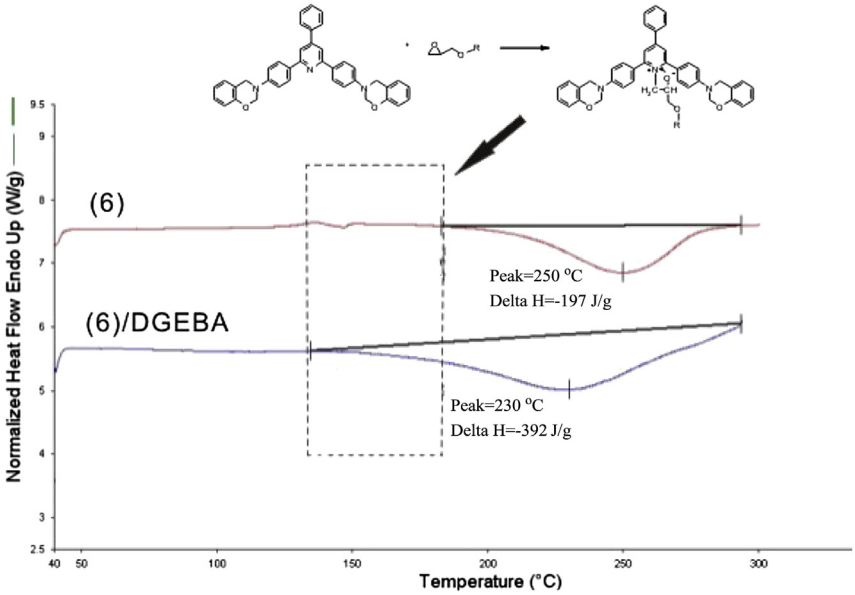

Fig. 6. DSC thermograms of (**6**) and (**6**)/DGEBA.

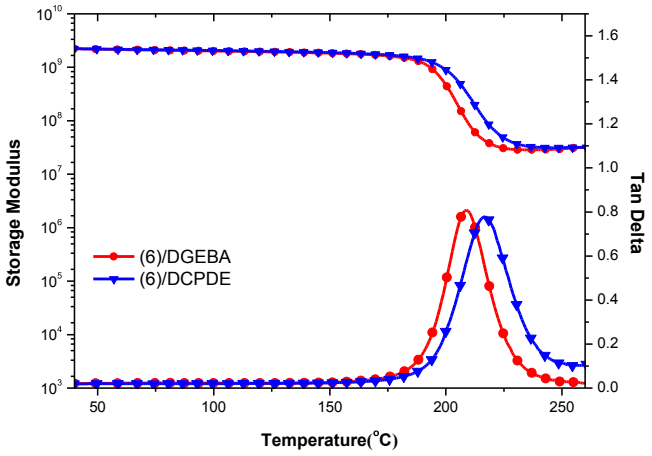

Fig. 7. DMA thermograms of the (**6**)/DGEBA and (**6**)/DCPDE thermosets.

solvents, (**7**) shows poor solubility in organic solvents. This result shows the advantage of the pyridinyl group in solubility. The poor solubility of (**7**) makes it difficult to process, which will be discussed below.

3.3. Curing of benzoxazine (*6*)

Fig. 2 shows the IR spectra of (**6**) after accumulative curing at each temperature for 20 min. The absorptions at 945, 1032, and 1232 cm^{-1} decreased gradually with the progress of curing, and disappeared completely after curing at 200 °C for 20 min. The Mannich-type C–N–C absorption at 1185 cm^{-1} and Ar–OH absorption at 1260 cm^{-1} appeared at a later stage of curing. This result suggests that *N,O*-acetal-type structure was formed at the initial stage of curing, and rearranged to Mannich-type structure, a thermodynamically more stable structure, at elevated temperatures [22–25]. This curing behavior was found in the catalyzed ring-opening of benzoxazine [22]. Since no extra catalyst was added in this system, a self-catalyzed characteristic was found. The unpaired electrons of the pyridinyl group are thought to be related with the self-catalyzed characteristic. Gu et al. also found a self-catalyzed phenomenon in the curing of a benzimidazole-containing benzoxazine [26]. Fig. 3 shows the DSC thermograms of (**6**) and (**7**). Compared with (**7**), a forward curing temperature was observed for (**6**). The result demonstrates the catalytic effect of pyridinyl moiety. Very recently, Takeichi et al. reported the synthesis of pyridinyl-containing benzoxazine monomer (B-3py) from bisphenol A, paraformaldehyde, and 3-aminopyridine [27]. They also found a forward curing temperature and attributed it to the catalytic effect on the basicity of the pyridinyl group. They proposed that the zwitterionic intermediate of ring-opened benzoxazine is stabilized by the basic pyridinyl group, thus accelerating the ring-opening polymerization at lower temperatures. Although the curing occurred, as supported by IR and DSC data, the preparation of void-free thermoset of (**6**) is not successful for unknown reasons.

3.4. Curing of (*6*)/epoxy

Fig. 4a shows the IR spectra of the (**6**)/DGEBA curing system. The epoxy absorption at 915 disappeared completely after curing at 160 °C. The characteristic absorptions at 945, 1032, and 1232 cm^{-1} disappeared gradually with the progress of curing. Unlike the curing of neat (**6**) (Fig. 2), the characteristic peaks of oxazine did not disappear completely in the (**6**)/DCPDE system after curing at 220 °C for 20 min, suggesting a slower curing rate. This result indicates that the catalytic effect of pyridinyl group on the curing of benzoxazine is not obvious, probably due to dilution effect when compared polymerization behaviors of benzoxazine/epoxy mixture with that of benzoxazine. Unexpectedly, a special carbonyl absorption at 1670 cm^{-1} was observed in Fig. 4a. A similar phenomenon was observed in the (**6**)/DCPDE system (Fig. 4b).

Xue and Ishida et al. studied the reactions between poly(4-vinyl pyridine) and epoxy resins [28–30]. They reported that the reactions include nucleophilic addition, Diels–Alder reaction, and rearrangement. The reactions led to pyridone or cyclic amide structure, as observed in the IR spectra at 1650 and a shoulder at 1670 cm^{-1}, respectively [28–30]. The order of reactivity of the pyridine derivate and epoxy is related with the structure of the pyridine derivate, where the order of reactivity is pyridine >> 2-methylpyridine > 2,6-dimethylpyridine [29]. The reactivity decreases rapidly with substituents in the ortho position of the pyridinyl group due to the steric hindrance of nucleophilic addition. In the case of the 2,6-dimethylpyridine, both positions adjacent to the nitrogen are occupied by the methyl group, and almost no reaction was observed in their reports. In this case, the two phenyl groups that are ortho to the nitrogen are expected to hinder the reaction between pyridinyl and epoxy resin. However, an absorption of

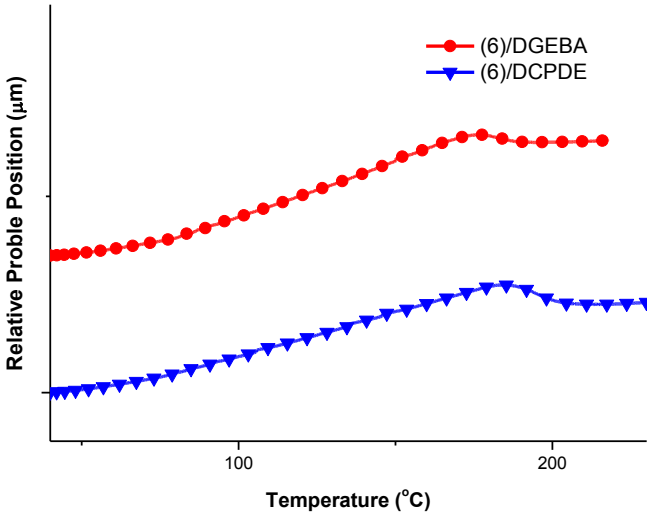

Fig. 8. TMA curves of the (**6**)/DGEBA and (**6**)/DCPDE thermosets.

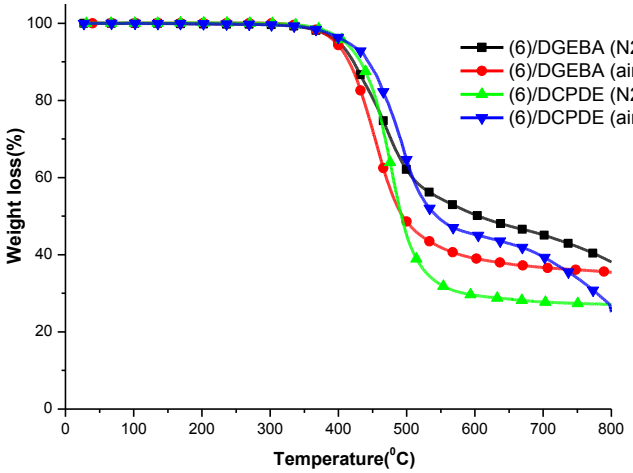

Fig. 9. TGA thermograms of (**6**)/epoxy in N_2 and air.

Table 3
Thermal properties of the (**6**)/DGEBA and (**6**)/DCPDE thermosets.

Curing system	E′ (GPa)[a]	Tan δ (°C) (DMA)[a]	T_g (°C) (TMA)[b]	CTE (ppm/°C)[c]	$T_{d5\%}$ (°C)[d]		Char yield[e]	
					N_2	air	N_2	air
(**6**)/DGEBA	2.19	209	175	51	396	400	38	35
(**6**)/DCPDE	2.20	217	185	48	410	414	27	25

[a] Measured by DMA at a heating rate of 5 °C/min; storage modulus (E′) are recorded at 50 °C; T_g was determined from the peak temperature of the tan δ curve.
[b] Measured by TMA at a heating rate of 5 °C/min.
[c] Coefficient of thermal expansion is recorded from 50 °C to 150 °C.
[d] Temperature corresponding to 5% weight loss by thermogravimetry at a heating rate of 20 °C/min in nitrogen and air.
[e] Residual weight % at 800 °C in nitrogen and air.

1670 cm^{-1} indicates that the reaction occurred, and the cyclic amide is the product of this system. Fig. 5 shows the ^{13}C NMR spectrum of (**6**)/DGEBA after curing at 140 °C and 180 °C (the same thermal treatment as those in Fig. 4). The spectrum is difficult to assign for each peak. However, a carbonyl signal at 192 ppm was observed after thermal treatment at 180 °C. The carbonyl signal, which was not seen after 140 °C treatment, supports the formation of cyclic amide. Fig. 6 shows DSC thermograms of (**6**)/epoxy. A forward exothermic peak was observed for (**6**)/epoxy when compared with that of (**6**). The forward exotherm is attributed to the nucleophilic addition of pyridinyl group to epoxy. According to Xue and Ishida [28–30], IR (Fig. 4), ^{13}C NMR (Fig. 5), and DSC data (Fig. 6), a reaction mechanism between (**6**) and epoxy is proposed in Scheme 2. Step I is the nucleophilic addition of the pyridinyl group on epoxy, forming an oxygen ion. Step II is the nucleophilic attack of the oxygen ion on the α-position of the pyridine, forming a conjugated diene after the aromatic structure of pyridine was destroyed. A Diels–Alder reaction is then carried out in step III for the conjugated diene. Finally, a cyclic amide was formed after the rearrangement in step IV. The rearrangement starts at temperatures higher than 160 °C, as supported by the appearance of carbonyl absorption in Fig. 4. Step V is the ring-opening of oxazine leading to crosslinking structure.

3.5. Thermal properties of benzoxazine/epoxy thermosets

Fig. 7 shows the DMA thermograms of the (**6**)/epoxy thermosets. Only one tan δ peak was observed, indicating that a homogeneous copolymer was obtained. The T_g obtained from the peak temperature of tan δ is 209 and 217 °C for the (**6**)/DGEBA and (**6**)/DCPDE thermoset, respectively. The value is relative high for benzoxazine/DGEBA-based thermosets. For example, the T_g of B-a/DGEBA is 154–175 °C, depending on the ratio of B-a and DGEBA [31]. Note that B-a is a benzoxazine based on bisphenol A/formaldehyde/aniline. This result demonstrates a high T_g characteristic of (**6**) as an epoxy curing agent. A possible reason is the difunctional benzoxazine (**6**) is acting as a trifunctional curing agent, since pyridinyl also acts as a curing site with epoxy resins, as shown in Scheme 2. Takeichi et al. reported that the T_g of pyridinyl-containing polybenzoxazine (PB-3py) is 40 °C higher than bisphenol A/formaldehyde/aniline-based polybenzoxazines (PB-a) due to the strong hydrogen bonding between the pyridinyl moiety and phenolic group [27]. However, no (**7**)/epoxy data are available for the comparison of properties in this work due to the poor solubility of (**7**) in epoxy and in organic solvents. TMA measurement (Fig. 8) shows the T_g value of (**6**)/DGEBA and (**6**)/DCPDE thermoset is 175 and 185 °C, respectively. Coefficient of thermal expansions (CTE) is 51 and 48 ppm/oC, respectively.

Fig. 9 shows the TGA thermograms of the (**6**)/DGEBA and (**6**)/DCPDE thermosets, with the results listed in Table 3. The 5% degradation temperature for (**6**)/DGEBA and (**6**)/DCPDE is 396 and 410 °C in nitrogen, and 400 and 414 °C in air, respectively. The values are relatively high when compared with the B-a/epoxy thermoset, which possesses 5% degradation temperature at 302–309 °C, dependent on the curing catalyst [32]. Takeichi et al. reported that pyridinyl-containing polybenzoxazine (PB-3py) has the same thermal stability as PB-a [27]. This result in Fig. 9 demonstrates that thermosets based on diamine-based benzoxazine display better thermal stability than thermosets based on bisphenol-based benzoxazine, which are consistent with those reported in our previous work [33].

4. Conclusions

We have successfully prepared a pyridinyl-containing benzoxazine (**6**) from the Mannich condensation of (**2**), phenol, and paraformaldehyde using toluene/ethanol as the reaction solvent. When cured with epoxy resins, the pyridinyl group provides solubility, as supported. An unexpected carbonyl absorption was observed at 1670 cm^{-1} in the IR spectrum. In addition, a carbonyl signal at 192 ppm was observed in the ^{13}C NMR spectrum. Referring to IR, DSC, and ^{13}C NMR data and the conclusion of Xue and Ishida [28–30], a reaction mechanism including nucleophilic addition, Diels–Alder reaction, rearrangement, and ring-opening of benzoxazine was proposed in the (**6**)/epoxy curing system. DMA data show T_g is as high as 209 and 217 °C for the (**6**)/DGEBA and (**6**)/DCPDE thermoset, respectively. The T_g value of 209 °C is relatively high for a thermosets based on DGEBA, showing a moderate-to-high T_g characteristic of (**6**) as an epoxy curing agent. A possible reason is the difunctional benzoxazine (**6**) is acting as a trifunctional curing agent, since pyridinyl also acts as a curing site with epoxy resins. Although the reactions between pyridine and epoxy have been reported [28–30], to the best of our knowledge, no literature has reported the reactions between epoxy and pyridinyl-containing benzoxazine with two bulky substitutions ortho to pyridinyl.

Acknowledgments

The authors thank the National Science Council of the Republic of China for financial support.

Appendix A. Supplementary data

Supplementary data related to this article can be found online at http://dx.doi.org/10.1016/j.polymer.2014.02.039.

References

[1] Ghosh NN, Kiskan B, Yagci Y. Prog Polym Sci 2007;32(11):1344–91.
[2] Ishida H, Agag T. Handbook of benzoxazine resins. Elsevier; 2011.
[3] Yagci Y, Kiskan B, Ghosh NN. J Polym Sci Part Polym Chem 2009;47(21):5565–76.
[4] Nair CPR. Prog Polym Sci 2004;29(5):401–98.
[5] Takeichi T, Agag T. High Perform Polym 2006;18(5):777–97.
[6] Ning X, Ishida H. J Polym Sci Part Polym Chem 1994;32(6):1121–9.

[7] Wang C-F, Su Y-C, Kuo S-W, Huang C-F, Sheen Y-C, Chang F-C. Angew Chem Int Ed 2006;45(14):2248–51.
[8] Tamami B, Yeganeh H. Polymer 2001;42(2):415–20.
[9] Wang K-L, Liou W-T, Liaw D-J, Huang S-T. Polymer 2008;49(6):1538–46.
[10] Tamami B, Yeganeh H. J Polym Sci Part Polym Chem 2001;39(21):3826–31.
[11] Liaw D-J, Wang K-L, Chang F-C, Lee K-R, Lai J-Y. J Polym Sci Part Polym Chem 2007;45(12):2367–74.
[12] Wang X, Li Y, Gong C, Zhang S, Ma T. J Appl Polym Sci 2007;104(1):212–9.
[13] Liaw D-J, Wang K-L, Chang F-C. Macromolecules 2007;40(10):3568–74.
[14] Chichibabin A, Zhur Zeide O. Russ Fiz Khim Obshch (J Russ Phys Chem Soc) 1914;46:1212.
[15] Frank RL, Seven RP. J Am Chem Soc 1949;71(8):2629–35.
[16] Li JJ. Chichibabin pyridine synthesis. Name reactions. Springer; 2009. pp. 107–9.
[17] Katritzky A, Rees C. Comprehensive heterocyclic chemistry, vol. 2. Oxford: Pergamon; 1984. p. 395.
[18] Weiss M. J Am Chem Soc 1952;74(1):200–2.
[19] Spiliopoulos IK, Mikroyannidis JA. Macromolecules 1998;31(4):1236–45.
[20] Lin CH, Chang SL, Shen TY, Shih YS, Lin HT, Wang CF. Polym Chem 2012;3(4):935–45.
[21] Kawaguchi AW, Sudo A, Endo T. J Polym Sci Part Polym Chem 2014;52(3):410–6.
[22] Sudo A, Kudoh R, Nakayama H, Arima K, Endo T. Macromolecules 2008;41(23):9030–4.
[23] Sudo A, Hirayama S, Endo T. J Polym Sci Part Polym Chem 2010;48(2):479–84.
[24] Wang YX, Ishida H. Polymer 1999;40(16):4563–70.
[25] Endo T, Sudo A. J Polym Sci Part Polym Chem 2009;47(19):4847–58.
[26] Yang P, Gu Y. J Polym Sci Part Polym Chem 2012;50(7):1261–71.
[27] Shibayama Y, Kawauchi T, Takeichi T. High Perform Polym; 2013. http://dx.doi.org/10.1177/0954008313495245.
[28] Xue G, Ishida H, Koenig JL. Die Makromol Chem Rapid Commun 1986;7(1):37–41.
[29] Xue G, Ishida H, Koenig JL. Polymer 1986;27(7):1134–7.
[30] Xue G, Ishida H, Koenig JL. Die Angew Makromol Chem 1986;142(1):17–27.
[31] Ishida H, Allen DJ. Polymer 1996;37(20):4487–95.
[32] Kimura H, Matsumoto A, Ohtsuka K. J Appl Polym Sci 2008;109(2):1248–56.
[33] Lin CH, Chang SL, Hsieh CW, Lee HH. Polymer 2008;49(5):1220–9.